Journal of Power Sources 196 (2011) 1802–1807

Contents lists available at ScienceDirect

Journal of Power Sources

journal homepage: www.elsevier.com/locate/jpowsour

Effect of cathode micro-porous layer on performance of anion-exchange membrane direct ethanol fuel cells

Y.S. Li, T.S. Zhao*, J.B. Xu, S.Y. Shen, W.W. Yang

Department of Mechanical Engineering, The Hong Kong University of Science and Technology, Clear Water Bay, Kowloon, Hong Kong, China

ARTICLE INFO

Article history:
Received 12 July 2010
Received in revised form 9 September 2010
Accepted 14 September 2010
Available online 1 October 2010

Keywords:
Direct ethanol fuel cell
Anion-exchange membrane
Water crossover
Micro-porous layer
Gas-diffusion layer
Carbon nanotubes

ABSTRACT

The effect of a cathode micro-porous layer that is composed of carbon powder or carbon nanotubes on cell performance is investigated. Polarization curves, together with the respective anode and cathode potentials, are measured. The results show that the cathode potential can be significantly improved with adding a hydrophobic micro-porous layer between the cathode catalyst layer and the gas-diffusion layer. The increased performance with the cathode micro-porous layer is mainly attributed to the fact that the cathode water flooding can be alleviated as a result of the reduced water crossover, which consequently facilitates the transport of oxygen to the catalyst layer. It is also found that a crack-free micro-porous layer made of carbon nanotubes gives a much higher cathode potential compared with a micro-porous layer composed of carbon powder.

© 2010 Elsevier B.V. All rights reserved.

1. Introduction

An anion-exchange membrane direct ethanol fuel cell (AEM DEFC) that uses a low-cost AEM, rather than a proton-exchange membrane (PEM), for direct methanol fuel cells (DMFCs), makes it possible to achieve faster electrokinetics of both the ethanol oxidation reaction (EOR) and oxygen reduction reaction (ORR), even with low-cost non-platinum metals as the electrocatalyst. The most important feature of the AEM DEFC is that ethanol is less toxic, has a higher energy density than methanol (6.1 vs. 4.6 kWh L^{-1}), and can be massively produced from agricultural products or biomass. In addition, the liquid-feed DEFC also possesses the same advantages as a DMFC, including simple system structure, high-specific energy and fast refueling [1–3]. For these reasons, AEM DEFCs have recently attracted increasing attention [4–10].

Past efforts on the development of AEM DEFCs have focused mainly on the development of advanced materials, including anion-exchange membranes and electrocatalysts, and the study of the mechanisms of both the EOR and ORR in alkaline media [11–20]. For example, Varcoe et al. [16] prepared a series of ETFE-based anion-exchange membranes with the radiation-grafting method. The tests showed that OH^- conductivity could be as high as 0.06 S cm^{-1} at 60 °C. Yanagi and Fukuta [17] tested the durability of a commercial A201 membrane made of the quaternary ammonium group and hydrocarbon polymer backbone in water and methanol at 80 °C, and indicated that the ion-exchange capacity (IEC) was stable for 2300 h. Shen et al. [18] compared Pd- and Pt-based catalysts for the EOR in alkaline media, and showed that Pd/C had a higher catalytic activity and better steady-state behaviour for ethanol oxidation than Pt/C. Chatenet et al. [19] reported that MnO_x/C electrocatalysts directed the ORR toward the four-electron pathway, and indicated that the rate-determining step was the second electron-transfer that involved the electrosplitting of the $O_{2,ads}$ species, yielding O_{ads} and hydroxide anion. Recently, Liang et al. [20] studied the mechanism of the EOR on a palladium electrode by means of cyclic voltammetry and found that the dissociative adsorption of ethanol proceeded somewhat faster and the rate-determining step was the removal of adsorbed ethoxi by adsorbed hydroxyl on the Pd electrode.

These have been relatively few investigations of mass transport behaviour in AEM DEFCs. One of the mass transport issues in acid proton exchange membrane fuel cells is water management, which aims to maintain a delicate balance between membrane dehydration and cathode flooding. In AEM DEFCs, however, a common conception is that cathode flooding is unlikely due to the fact that water is consumed as a reactant at the cathode and the electro-osmotic drag (EOD) moves water from the cathode to anode. Recently, the authors' work [21] has shown that cathode flooding also occurs in an AEM DEFC, primarily because the diffusion flux from the anode to the cathode outweighs the total water flux due to the both ORR and EOD. Therefore, avoiding cathode flooding is a water management issue in AEM DEFCs. Being moti-

* Corresponding author. Tel.: +852 2358 8647; fax: +852 2358 1543.
E-mail address: metzhao@ust.hk (T.S. Zhao).

0378-7753/$ – see front matter © 2010 Elsevier B.V. All rights reserved.
doi:10.1016/j.jpowsour.2010.09.077

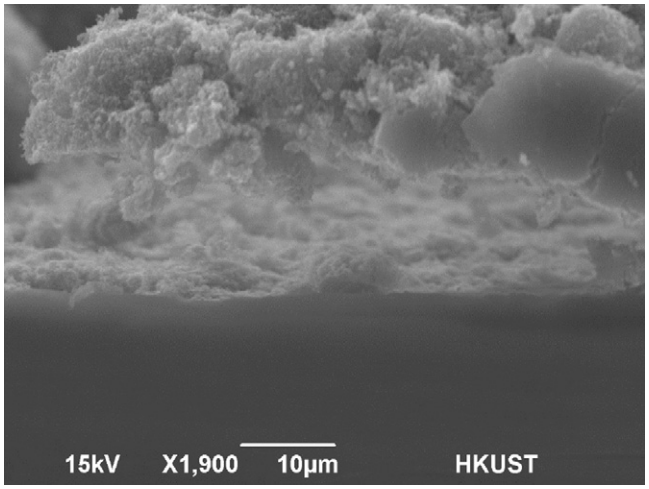

Fig. 1. SEM images of cross-sectional view of prepared catalyst-coated MEA.

vated by this need, this study examines the effect of the cathode MPL design on cathode flooding behaviour and cell performance in an AEM DEFC.

2. Experimental

2.1. Preparation of MEA

An in-house fabricated DEFC which consisted of a membrane–electrode assembly (MEA) with an active area of 2.0 cm × 2.0 cm sandwiched between a pair of current-collectors that were held by two fixture plates. The MEA was composed of an anion-exchange membrane (A201, Tokuyama), a commercial anode electrode with non-platinum HYPERMECTM catalysts (Acta) and a cathode catalyst layer (CL). The CL was fabricated in-house by the catalyst-coated membrane (CCM) method; namely, catalyst inks were prepared by mixing non-platinum HYPERMEC™ K14 catalysts at a loading of 2.0 mg cm^{-2} and an A3 ionomer (Tokuyama) with 1-propanol as the solvent. The catalyst inks were stirred continuously in an ultrasonic bath for 10 min to ensure that they were well-dispersed. The content of the A3 as a binder in the cathode catalyst layer was maintained at about 5 wt.%. Subsequently, the well-dispersed catalyst inks were directly sprayed on to one side of the membrane with a spray gun. The prepared MEA was heat-treated in a vacuum oven at 70 °C for 30 min to remove residual organic solvents. A scanning electron micrograph of the cross-sectional view of the prepared MEA is presented in Fig. 1. The cathode CL is in intimate contact with the membrane and this confirms that the anion-exchanger membrane-based MEA can be well prepared by the CCM method, with which the effect of different cathode MPL designs can be investigated by keeping the other MEA components, including the anode electrode, the membrane, and the cathode CL, unchanged. MPLs with different polytetrafluoroethylene (PTFE) loadings and different carbon (Vulcan XC-72 carbon powder or carbon nanotube) loadings were prepared and applied to the same backing layer (Toray-090 carbon paper) without wet-proofing treatment.

2.2. Current-collectors

Both the anode and cathode fixture plates were made of stainless-steel. A single serpentine flow-field, with a 0.5 mm channel depth, a 1.0 mm channel width, and a 1.0 mm rib width, was machined on one side of each fixture plate. In addition, to visualize two-phase transport behaviour in the cathode flow-field, a fixture made of transparent poly methyl methacrylate (PMMA) was covered on a serpentine current-collector plate.

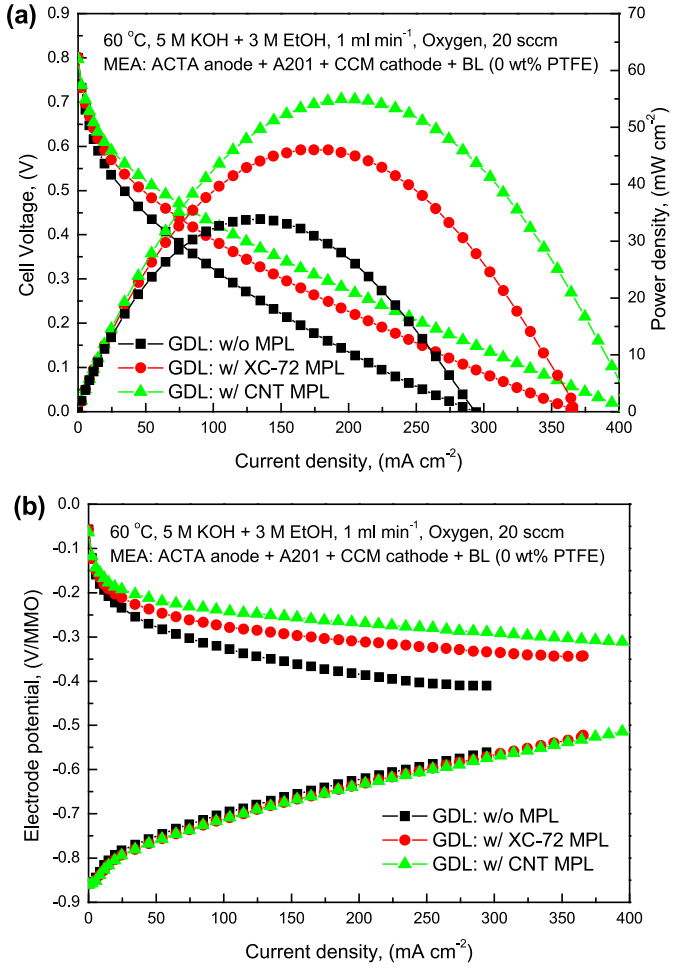

Fig. 2. Effect of cathode MPL on (a) cell performance and (b) electrode potentials.

2.3. Measurement instrumentation and test conditions

Experiments were conducted in the cell test station detailed elsewhere [15]. Tests of AEM DEFC voltage-current (polarization) curves were controlled and measured by an electric load system (Arbin BT2000, Arbin Instrument Inc.). At the anode, an aqueous solution, containing 3.0 M ethanol and 5.0 M KOH, was supplied by a peristaltic pump at a flow rate of 1.0 ml min^{-1}. At the cathode, 99.5% oxygen at ambient pressure with a flow rate of 20 standard cubic centimeters per minute (sccm) was fed without humidification. A mass-flow controller (Omega FMA-78P4), along with a multiple-channel indicator (Omega FMA-765A), was used to control and measure the oxygen flow rate. Before entering the fuel cell, the aqueous solution and oxygen were preheated by the electrical heating rods that were installed in both the anode and cathode fixture plates. The cell operating temperature, set at 60 °C, was measured with a thermocouple installed at the anode fixture plates. The cell resistance, R, was determined by a d.c.-pulse method. The anode potential was measured by an Hg|HgO|KOH (1.0 M) (MMO, 0.098V vs. SHE) reference electrode [22]. Subsequently, the cathode potential was obtained by added the anode potential to the iR-corrected cell voltage. The morphology of the catalyst-coated membrane and the cathode GDL was examined with a scanning electron microscope (SEM, JEOL-6390).

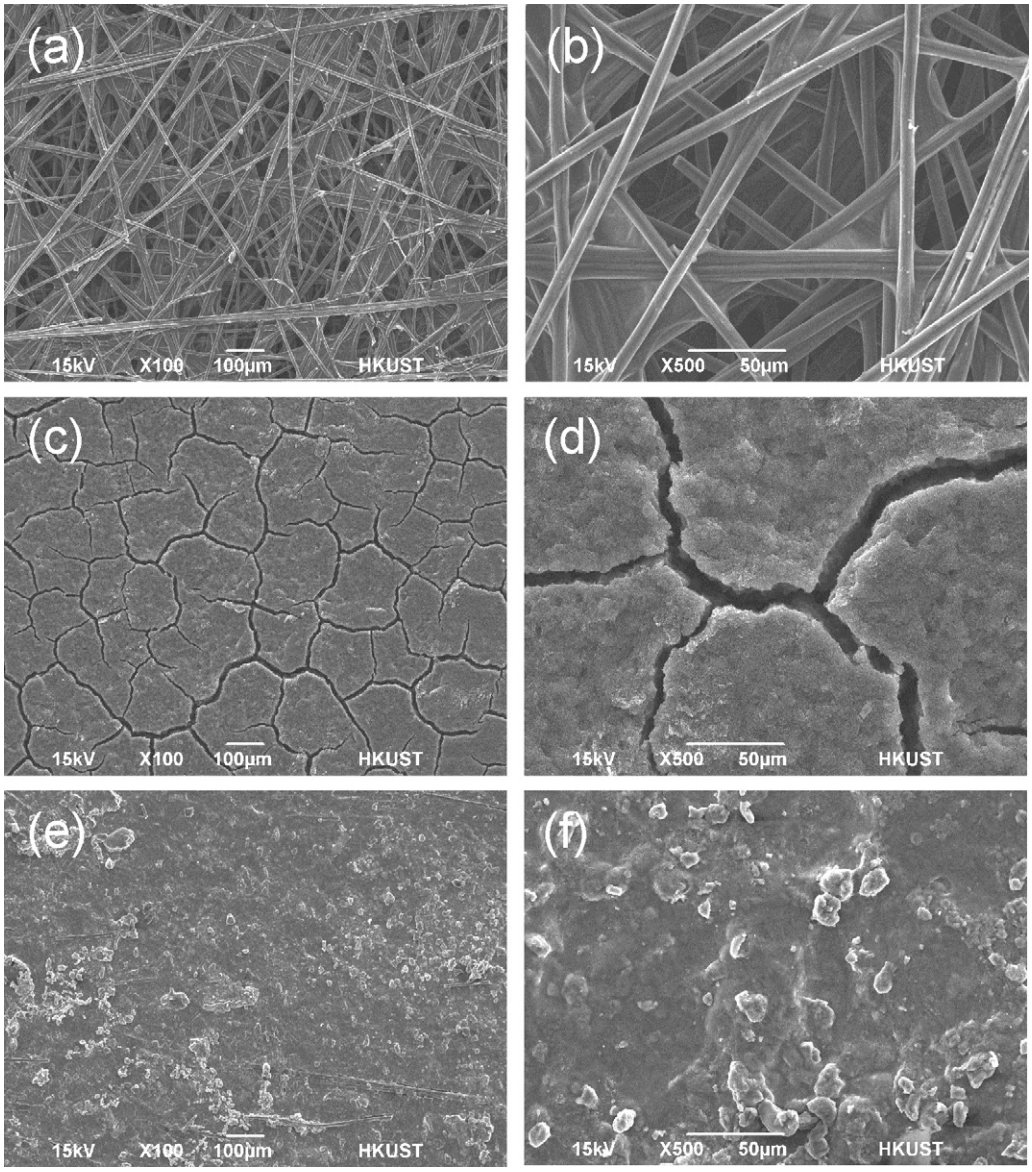

Fig. 3. Surface morphologies of GDLs: (a and b) carbon paper without MPL, (c and d) carbon-powder MPL, and (e and f) nanotube MPL.

2.4. Determination of water-crossover flux

In an AEM DEFC, liquid water in the aqueous solution fed to the anode, along with that produced from the EOR, can diffuse through the membrane to the cathode CL, where part of it reacts with oxygen to form hydroxide ions, and the remainder is transported through the cathode DL to the cathode flow-field. Simultaneously, water can also be dragged by the migration of OH^- from the cathode to the anode. The authors' recent work [21] showed that under typical operating conditions a net water flux permeates through the membrane from the anode to the cathode, which is termed as the water-crossover flux. As part of the water-crossover flux, J_{wc}, is consumed by the ORR at the cathode CL according to

$$J_{ORR} = \frac{i}{2F} \tag{1}$$

where F is Faraday's constant and i is the discharge current density, while the remainder goes to the cathode, which is represented by [23,24]:

$$J_{GDL} = \frac{N_{H_2O}}{A} \tag{2}$$

where N_{H_2O} denotes the rate of water collected at the exit of the cathode flow channel and A represents the electrode surface area. Hence, the water-crossover flux can be determined by summing Eqs. (1) and (2) to give:

$$J_{wc} = J_{ORR} + J_{GDL} \tag{3}$$

To determine the rate of water collected at the exit of the cathode flow channel, N_{H_2O}, a water trap filled with anhydrous $CaSO_4$ (Dryerite®) was installed at the exit [23,24]. By weighing the water trapped over a specified period at a given current density, the flow rate of water at the cathode outlet, N_{H_2O}, can be determined. Thirty minutes were needed to achieve a steady-state condition before collecting the water. The back pressures of both the anode and cathode electrodes were maintained at the atmosphere pressure during the test to eliminate the influence of back pressure on water transport.

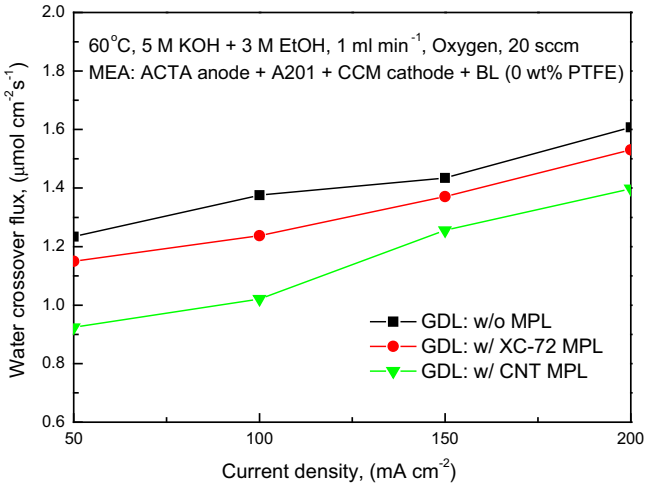

Fig. 4. Effect of MPL design on water-crossover flux.

3. Results and discussion

3.1. Effect of micro-porous layer

The performance of the DEFC with various GDLs is shown at Fig. 2a. Three cases were studied: the GDL without an MPL, the GDL with a MPL made of XC-72 carbon powder, and the GDL with a MPL made of CNTs. Clearly, it is seen that the cell performance is improved significantly by including a hydrophobic MPL at the cathode. It is also noticed that the cell performance is much higher with the MPL made of CNTs than that with the MPL made of carbon powders. The peak power density increased from 34 to 46 mW cm^{-2} when the MPL made of carbon powder was included; it further increased to 55 mW cm^{-2} when the MPL made of nanotubes was used. The respective anode and cathode potentials are shown in Fig. 2b. It is seen that the anode potential almost remains the same for all the cases studied, whereas the cathode potential increases with the addition of the MPL, especially with the MPL made of CNTs. This fact suggests that the increased cell performance when including a cathode MPL is due to the increased cathode potential that can be explained as follows. Images of the surface morphology of the original cathode backing layer without and with the MPL are presented in Fig. 3. The addition of the MPL substantially reduces the mean pore size of the porous layer. In addition, because of the hydrophobic nature of the PTFE-treated MPL, a much higher hydraulic liquid pressure can be built up in the cathode, which enables a reduction in water crossover and hence alleviates the cathode flooding problem. As a result, the cathode potential is increased because of the enhanced oxygen transport. It is also noticed from Fig. 3c and d that some macropores between 2.0 and 20.0 μm, or so-called mud cracks, are formed on the surface of the MPL made of carbon powder [24–26]. The formation of these large cracks can reduce the liquid pressure, and thereby enhance the water-crossover flux. On the other hand, however, it is found from the images in Fig. 3e and f that the MPL made of CNTs is totally free of large cracks [27]. This is why the cathode potential for the MPL made of CNTs is higher than that for the MPL made of carbon powders. As shown in Fig. 4, the rate of water crossover can be greatly lowered by adding a hydrophobic MPL at the cathode. More importantly, it is shown that the rate of water crossover is much lower for the MPL made of CNTs as compared with that for the MPL made of carbon powders.

In summary, the above experimental results indicate that the presence of the hydrophobic MPL at the cathode GDL in an AEM DEFC can significantly enhance cell performance, mainly because

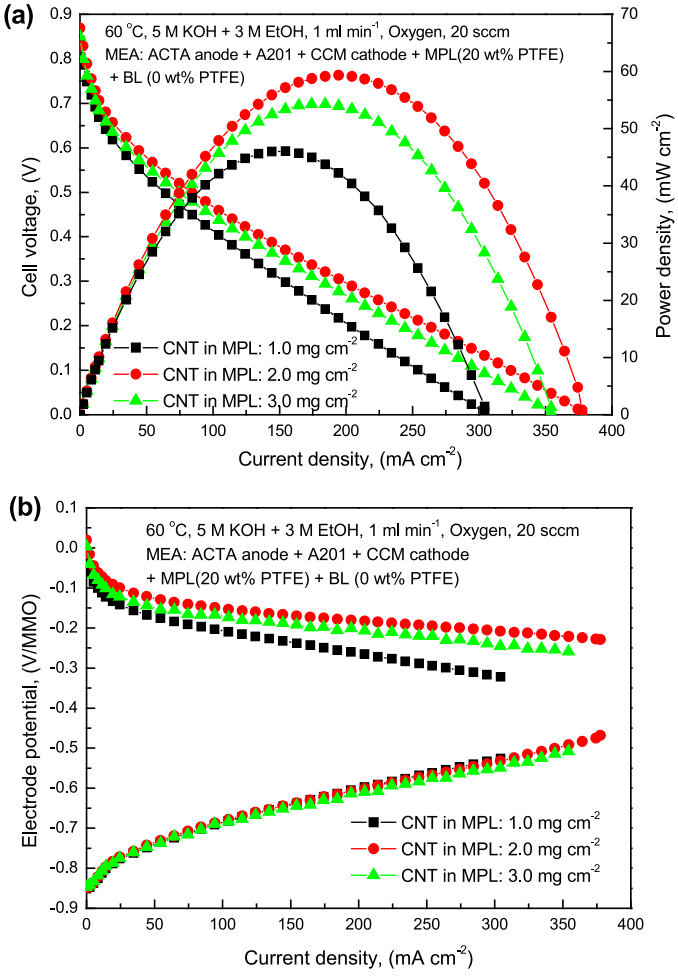

Fig. 5. Effect of CNT loading at cathode MPL on (a) cell performance and (b) electrode potentials.

introducing the hydrophobic MPL decreases the permeability and liquid saturation of the cathode GDL, which tends to alleviate the cathode flooding and hence to enhance oxygen transport with a resulting improvement in performance. Therefore, as in other acid DMFCs and DEFCs, a cathode MPL is also essential in AEM DEFCs.

3.2. Effect of CNT loading

The effect of the CNT loading on cell performance was investigated by testing the different MPLs, which consisted of the same PTFE loading (20 wt.%) but different CNT loadings. The same PTFE loading ensures that the hydrophobic level and the porosity of the MPLs does not change with CNT loading. Hence, increasing the CNT loading means an increase in the thickness of the MPL. It is seen from Fig. 5a that the cell performance increases when the CNT loading is increased from 1.0 to 2.0 mg cm^{-2}, but it decreases when the loading is increased further to 3.0 mg cm^{-2}. The best cell performance is achieved at a CNT loading of 2.0 mg cm^{-2}. The data in Fig. 5b indicate that the variation in cell performance with the CNT loading is due to the change in cathode potential because the anode potential remains almost the same when the CNT loading is varied. This behaviour can be explained as follows. On one hand, increasing the CNT loading in the MPL increases the MPL thickness and hence reduces the rate of water crossover. This can be confirmed by the measured rate of water crossover shown in Fig. 6. At 200 mA cm^{-2}, the rate of water crossover is reduced from 1.5 to 1.1 μmol cm^{-2} s^{-1} when the CNT loading is increased from 1.0

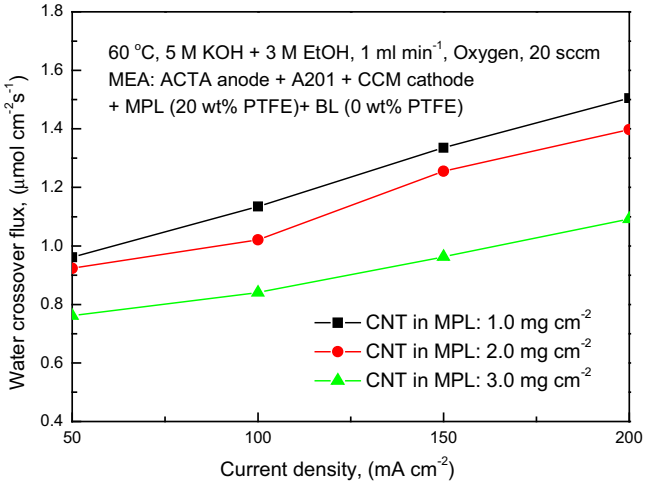

Fig. 6. Effect of CNT loading in cathode MPL on water-crossover flux.

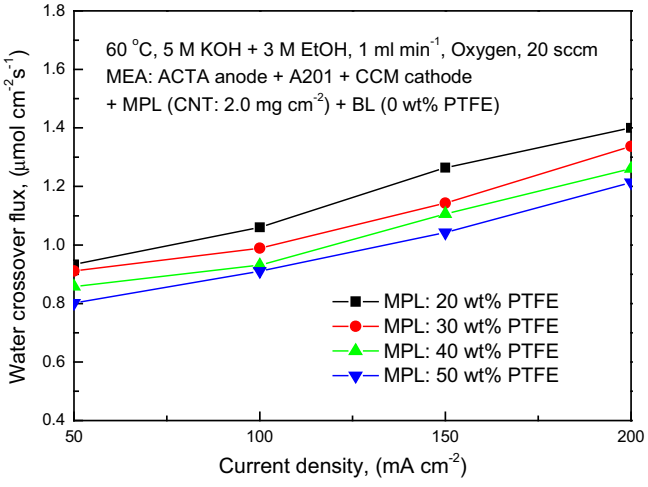

Fig. 8. Effect of PTFE loading in cathode MPL on water-crossover flux.

to 3.0 mg cm^{-2}. Accordingly, the cathode flooding problem can be alleviated and hence oxygen transport can be enhanced. On the other hand, an increase in the thickness of the MPL increases the transport resistance of oxygen. Therefore, the CNT loading should be maintained at an optimum level such that the cell performance can be maximized.

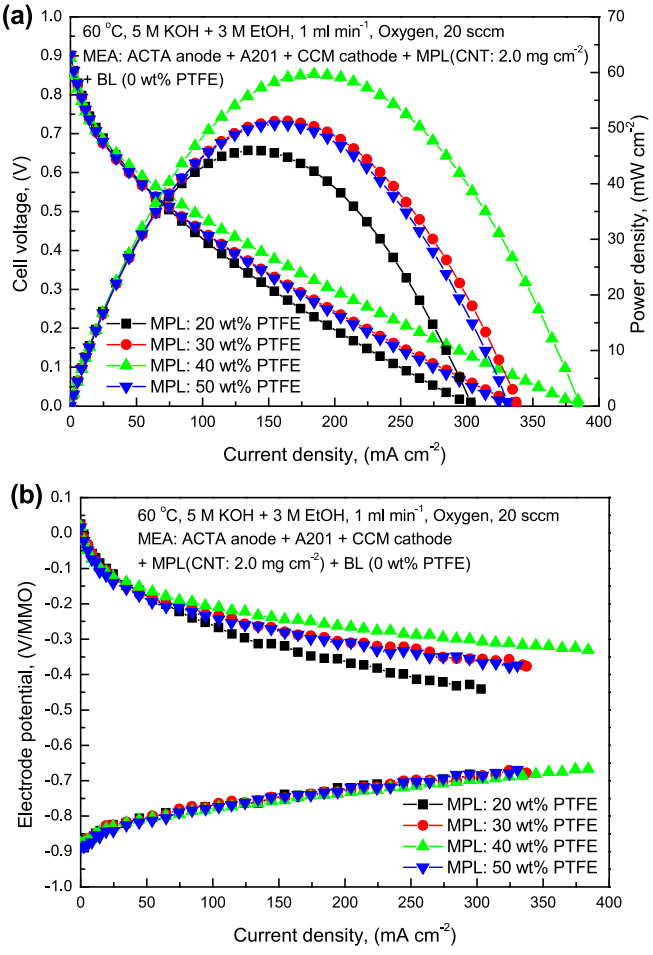

Fig. 7. Effect of PTFE loading in cathode MPL on (a) cell performance and (b) electrode potentials.

3.3. *Effect of PTFE loading*

In addition to the CNT loading, the effect of PTFE loading on cell performance was also studied by testing the different MPLs, with the same CNT loading (2.0 mg cm^{-2}) but different PTFE loadings. The same CNT loading indicates that the thickness of the MPL does not change with PTFE loading. The effect of PTFE loading in the MPL on cell performance is displayed in Fig. 7a. When increasing the PTFE loading from 20 to 40 wt.%, the cell performance is significantly increased. For instance, the peak power density increases from 45 to 60 mW cm^{-2} as the PTFE loading increases from 20 to 40 wt.%. It is found, however that further increase in PTFE loading from 40 to 50 wt.% causes a decrease in cell performance. A peak power density of about 60 mW cm^{-2} is achieved at a PTFE loading of 40 wt.%. Measurement of the electrode potentials also indicates that the effect of PTFE loading on cell performance is mainly attributed to the change in cathode potential, as indicated in Fig. 7b. The reason why there exists an optimum PTFE loading to achieve the best cell performance can be explained as follows. On one hand, an increase in PTFE loading increases the hydrophobic level so as to reduce the water crossover, as indicated in Fig. 8, leading to the better oxygen transport in the cathode. On the other hand, a higher PTFE loading lowers the porosity of the MPL and reduces the connectivity of pores in the MPL which, in turn, hinders transport of oxygen to the catalyst layer. As a result, there exists an optimum PTFE loading in the MPL for the best cell performance.

4. Conclusions

In an alkaline membrane based DEFC, cathode flooding occurs because of the fact that the diffusion flux from the anode to the cathode outweighs the total water flux due to the ORR and EOD. Hence, avoiding cathode flooding is a water management issue in AEM DEFCs. Being motivated by this need, a study has been made of the effect of cathode MPL design on cathode flooding behaviour and cell performance in an AEM DEFC. Salient findings and conclusions are as follows:

(1) The presence of a hydrophobic MPL at the cathode GDL in an AEM DEFC can improve cell performance, because introducing the hydrophobic MPL can decrease water crossover from the anode to the cathode, and hence can enhance oxygen transport. This suggests that as in other acid DMFCs and DEFCs, a cathode MPL is an essential component of an AEM DEFC.

(2) Performance tests indicate that a MPL made of CNTs exhibits higher cell performance than a MPL made of carbon powder.
(3) The loadings of both CNT and PTFE in the cathode MPL not only affect water crossover but also influence oxygen transport. Appropriate CNT and PTFE loadings are essential to achieve a balance between reduced water crossover and increased oxygen transport resistance. The presently configured cathode MPL with a CNT loading of 2.0 mg cm^{-2} and a PTFE loading of 40-wt.% is found to produce the best cell performance.

Acknowledgement

The work was fully supported by a grant from the Research Grants Council of the Hong Kong Special Administrative Region, China (Project No. 623709). The material support from Acta and Tokuyama is greatly acknowledged.

References

[1] X. Ren, W. Henderson, S. Gottesfeld, J. Electrochem. Soc. 144 (1997) 267–270.
[2] Q. Ye, T.S. Zhao, J.G. Liu, Electrochem. Solid State Lett. 8 (2005) A549–A553.
[3] S.C. Thomas, X. Ren, S. Gottesfeld, J. Electrochem. Soc. 146 (1999) 4354–4359.
[4] C. Bianchini, P.K. Shen, Chem. Rev. 109 (2009) 4183–4206.
[5] E. Antolini, E.R. Gonzalez, J. Power Sources 195 (2010) 3431–3450.
[6] Z. Ogumi, K. Matsuoka, S. Chiba, M. Matsuoka, Y. Iriyama, T. Abe, M. Inaba, Electrochemistry 70 (2002) 980–983.
[7] Y.S. Li, T.S. Zhao, Z.X. Liang, J. Power Sources 190 (2009) 223–229.
[8] C. Bianchini, V. Bambagioni, J. Filippi, A. Marchionni, F. Vizza, P. Bert, A. Tampucci, Electrochem. Commun. 11 (2009) 1077–1080.
[9] L.H. Jiang, G.Q. Sun, S.G. Sun, J.G. Liu, S.H. Tang, H.Q. Li, B. Zhou, Q. Xin, Electrochim. Acta 50 (2005) 5384–5389.
[10] A.D. Modestov, M.R. Tarasevich, A.Y. Leykin, V.Y. Filimonov, J. Power Sources 188 (2009) 502–506.
[11] E.H. Yu, K. Scott, R.W. Reeve, Fuel Cells 3 (2003) 169–176.
[12] L.D. Zhu, T.S. Zhao, J.B. Xu, Z.X. Liang, J. Power Sources 187 (2009) 80–84.
[13] M.A. Kostowskyj, D.W. Kirk, S.J. Thorpe, Int. J. Hydrogen Energy 35 (2010) 5666–5672.
[14] J.R. Varcoe, R.C.T. Slade, Fuel Cells 5 (2005) 187–200.
[15] Y.S. Li, T.S. Zhao, Z.X. Liang, J. Power Sources 187 (2009) 387–392.
[16] J.R. Varcoe, M. Beillard, D.M. Halepoto, J.P. Kizewski, S.D. Poynton, R.C.T. Slade, ECS Trans. 16 (2008) 1819–1834.
[17] H. Yanagi, K. Fukuta, ECS Trans. 16 (2008) 257–262.
[18] C.W. Xu, P.K. Shen, Y.L. Liu, J. Power Sources 164 (2007) 527–531.
[19] I. Roche, E. Chainet, M. Chatenet, J. Vondrak, J. Phys. Chem. C 111 (2007) 1434–1443.
[20] Z.X. Liang, T.S. Zhao, J.B. Xu, L.D. Zhu, Electrochim. Acta 54 (2009) 2203–2208.
[21] Y.S. Li, T.S. Zhao, R. Chen, J. Power Sources 196 (2011) 133–139.
[22] E.H. Yu, K. Scott, Electrochem. Commun. 6 (2004) 361–365.
[23] Y.S. Li, T.S. Zhao, W.W. Yang, Int. J. Hydrogen Energy 35 (2010) 5656–5665.
[24] C. Xu, T.S. Zhao, Y.L. He, J. Power Sources 171 (2007) 268–274.
[25] H.K. Lee, J.H. Par, D.Y. Kim, T.H. Lee, J. Power Sources 131 (2004) 200–206.
[26] J. Yu, M.N. Islam, T. Matsuura, M. Tamano, Y. Hayashi, M. Hori, Electrochem. Solid State Lett. 8 (2005) A320–A323.
[27] A.M. Kannan, V.P. Veedu, L. Munukutla, M.N. Ghasemi-Nejhad, Electrochem. Solid State Lett. 10 (2007) B47–B50.